

NewSOL Project (720985)

Thermocline degradation

Pedro Azevedo

August, 2021

Copyright notice

LEN-UEREE-2021-N01-IR

“Thermocline degradation”

Internal Report on work developed by LNEG included in Task 6.3 “Test monitoring of TES system prototypes” for partial fulfillment of deliverable D6.2 “Test operation of the thermocline concrete tank and the modular concrete”.

Azevedo, Pedro

August, 2021

Copyright @ 2021 by LNEG. All rights reserved. The contents of this document (e.g., texts, graphics, photos, logos, etc.) and the document itself are protected by copyright. This document has been prepared by LNEG. Any distribution or presentation of the content is prohibited without prior written consent by LNEG.

Without the written authorization by LNEG this document and/or parts thereof must not be distributed, modified, published, translated, or reproduced, neither in form of photocopies, microfilming nor other – especially electronic – processes. This provision also covers the inclusion into or the evaluation by databases. Contraventions will entail legal prosecution.

The advice and strategies contained herein may not be suitable for every situation. You should consult with a professional where appropriate. Neither the institution nor author shall be liable for any loss of profit or any other commercial damages, including but not limited to special, incidental, consequential, or other damages in case of misuse of the information contained herein.

Table of contents

Copyright notice	2
Table of contents	3
List of figures	4
List of tables	4
1. Introduction.....	5
2. Control scheme.....	5
3. Prototype TCT performance	6
4. Prototype TCT performance (alternate strategy).....	11
5. Upscaled TCT performance (alternate strategy).....	14
6. System Advisory Model (SAM)	20
7. Conclusions	20

List of figures

Figure 1: Schematic diagram of a CSP plant with direct thermocline tank storage with bypass to prevent low temperature molten salts to be feed to the power block.....	6
Figure 2: Schematic diagram of a CSP plant with direct thermocline tank storage with bypass to prevent low temperature molten salts to be feed to the power block.....	7
Figure 3: Temperature profiles along the axial axis of the TCT over the course of 24 charging/discharging cycles.....	8
Figure 4: Operation time, for both the charge and the discharge operations, over 24 cycles.....	9
Figure 5: Stored energy vs Cycle number, after charge and discharge operations, for both $m=5,373$ kg/s and $m=3,2238$ kg/s.....	10
Figure 6: Output temperature for 24 consecutive cycles during the discharge operation ($m=5,373$ kg/s)....	10
Figure 7: Temperature profiles along the axial axis of the TCT over the course of 12 charging/discharging cycles.....	11
Figure 8: Operation time, for both the charge and the discharge operations, over 12 cycles.....	12
Figure 9: Stored energy vs Cycle number, after charge and discharge operations, for $m=5,373$ kg/s.	13
Figure 10: Output temperature for 12 consecutive cycles during the discharge operation ($m=5,373$ kg/s).	14
Figure 11: Temperature profiles along the axial axis of the upscaled TCT over the course of 6 charging/discharging cycles.....	17
Figure 12: Operation time, for both the charge and the discharge operations, over 6 cycles.....	17
Figure 13: Stored energy vs Cycle number, after charge and discharge operations, for $m=319,8$ kg/s.....	19
Figure 14: Output temperature for 6 consecutive cycles during the discharge operation ($m=319,8$ kg/s)....	19

List of tables

Table 1: Main specifications of the TCT.....	7
Table 2: Stored energy in the TCT considering the theoretical values, the Cycle 1 values, and the Cycle 24 values, in the end of both the charge and discharge operations.....	9
Table 3: Stored energy in the TCT considering the theoretical values, the Cycle 1 values, and the Cycle 12 values, in the end of both the charge and discharge operations.....	13
Table 4: Main specifications for the upscaled TCT.....	15
Table 5: Stored energy in the upscaled TCT considering the theoretical values, the Cycle 1 values, and the Cycle 6 values, after both the charge and discharge operations.....	18

1. Introduction

According to Task 6.3 of DOA, LNEG was supposed “to define an appropriate monitoring scheme and set of tests to collect the experimental data from the thermocline tank (TCT), necessary to the evaluation of the thermodynamic performance of the prototype and improvement and validation of the computational models”.

However, due to known delays on the construction phase of the thermocline tank, the experimental period and its related data is not available, at the moment. Nevertheless, although the validation of the computational models was not possible, some additional adaptations to the models and analysis were developed that can impact namely the assessment of the cycling effect over effective thermal capacity, including for an upscaled solution.

This report approaches the problem of the thermocline tank (TCT) degradation that can develop after consecutive cycles. Besides the control strategy, calculations were performed towards the assessment of the prototype TCT performance considering the control scheme disclosed in D7.9¹ and in some literature². An alternate operation strategy is proposed, and its performance assessed and, finally, an upscaled TCT, also disclosed in D7.9, is also assessed considering the alternate operation strategy.

Additionally, comments with regard to the model used in the System Advisory Model (SAM)³, also disclosed in D7.9, namely its thermocline related shortcomings, are made.

2. Control scheme

Depending on the chosen operating strategies and in order to analyze the thermocline performance, one of the initial tasks is to simulate the cyclic performance of the TCT. Although full charge and discharge of the thermocline is desirable from the point of view of TES occupancy factor and overall plant yield, usually, in real cases, this not possible due to technical limitations.

Possibly the main constraint is the minimum discharging temperature because it is limited by the accepted temperature to the power cycle. Although the recycling of the TCT at the end of the discharge operation can still be possible, if a bypass is considered (Figure 1), the inclusion of this component can be avoided if the recycling of the TCT is considered in the end of a charge operation.

¹ T. Eusébio et al. (2021), “Technical-Economical Assessment of the NEWSOL thermal storage concepts: Thermocline”, Deliverable D7.9, NewSOL project, University of Évora, August, 2021.

² F. Núñez et al. (2019), “Analysis of steel making slag pebbles as filler material for thermocline tanks in a hybrid thermal energy storage system”, *Solar Energy* 188 (2019) 1221–1231.

³ National Renewable Energy Laboratory, “System Advisor Model (SAM), Version 2013.9.20.” [Online]. Available: <https://sam.nrel.gov/>. [Accessed: 08-Apr-2020].

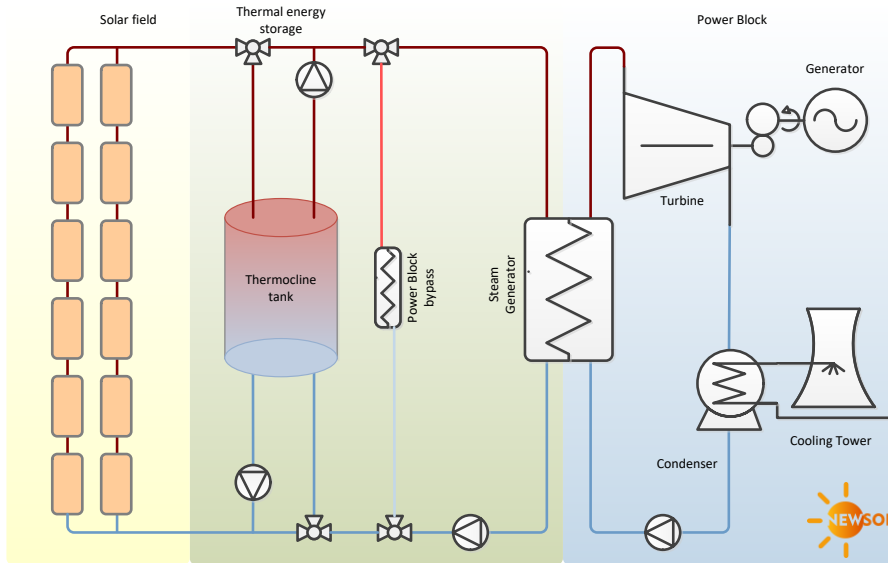


Figure 1: Schematic diagram of a CSP plant with direct thermocline tank storage with bypass to prevent low temperature molten salts to be feed to the power block.

However, this document presents the analysis of several conditions, as presented in D7.9 and others including the approach to the possibility of not recycling the TCT during regular operation cycles.

Considering the experimental limitations to theoretically fully charge and discharge the TCT, The proposed operation strategy considers a 30 °C temperature difference to limit both the charge and discharge periods. Thus, during the thermocline tank charge operation, the temperature at the bottom of the tank is monitored, and when the temperature increases by 30 °C, the charge process ends and immediately the discharge operation starts. During the discharge operation, the variable that controls the duration of the discharge is the temperature at the top outlet. When the outlet temperature drops by 30 °C the discharge process stops, and the cycle starts again.

3. Prototype TCT performance

The daily cycle described in D5.1⁴ included 1 charging period (4h), 1 discharging period (4h) and 2 idle periods (8h each, one before the charging period and the other after the discharging period). Considering the design mass flow of 5,373 kg/s, the tank is theoretically fully charged⁵ in less than 2,5h (slightly less for the discharge operation), despite the charging period of 4h. Table 1 presents the main specifications of the TCT.

⁴ P. Azevedo et al. (2019), "System configuration for thermocline concrete tank", Deliverable D5.1, NewSOL project, LNEG, January, 2019.

⁵ Theoretical fully charge means that the outlet temperature matches the inlet temperature. The same applies to theoretical fully discharge.

Table 1: Main specifications of the TCT

Description	Units	Value
Tank height	[m]	3,825
Tank internal diameter	[m]	2,9
Maximum temperature	[°C]	500
Minimum temperature	[°C]	180
Local porosity	[%]	50
Global porosity	[%]	67,23

If a lower mass flow is considered, as described in D5.1 (60% of the design mass flow), the tank shall need roughly 3,5h to be charged. Nevertheless, the tank would be fully charged and fully discharged after the charge and discharge period, respectively.

According to the proposed operation strategy, Figure 2 shows the temperature along the packed-bed axial axis at the end of both the charge and the discharge operations considering the design point mass flow. The axial axis is 3,825m at the top of the tank and it decreases until the bottom of the tank (0 m).

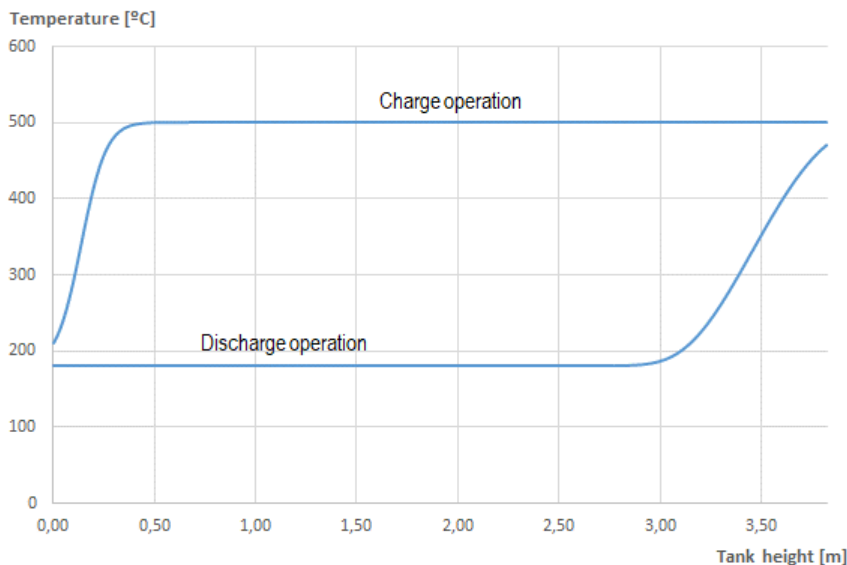


Figure 2: Schematic diagram of a CSP plant with direct thermocline tank storage with bypass to prevent low temperature molten salts to be feed to the power block.

As described by Núñez et al², consecutive charging/discharging cycles of the TCT impact the internal temperature gradient distribution along time, changing the thermocline depth and, therefore, its ability to deliver heat over a minimum temperature threshold at the power block inlet. This effect is illustrated in Figure 3, with the temperature profiles along the axial axis of the TCT over the course of 24 charging/discharging cycles.

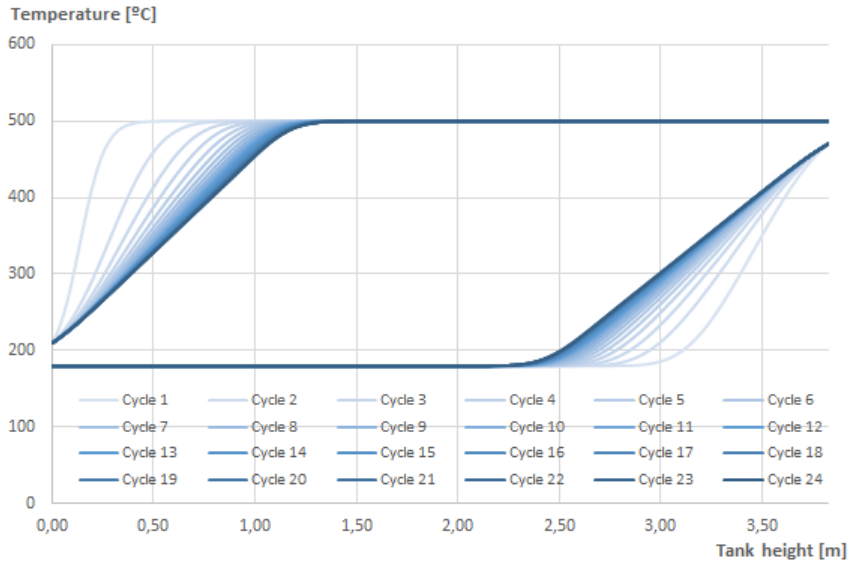


Figure 3: Temperature profiles along the axial axis of the TCT over the course of 24 charging/discharging cycles.

It can be observed that the temperature profiles converge with the number of cycles for both the charge and the discharge operations. As mentioned previously, it can be observed that the difference of the temperature profiles at the end of the discharge or charge process between a cycle and its previous decreases, while the number of cycles increases, and the temperature profiles converge. The considered 24 cycles represent a convergence criterion lower than 0,05% variation, on the total amount of energy stored in the tank, using the previous cycle as reference. For the purpose of this study, the reference temperature was the minimum temperature considered for the Yara MOST molten salts (180 °C). This way, if the tank is fully discharged, isothermal at the minimum temperature, the stored energy yields zero. Table 2 presents the stored energy in the TCT considering the theoretical values, the Cycle 1 values, and the Cycle 24 values, in the end of both the charge and discharge operations. From Table 2 is also possible to foresee that, without recycling the TCT, the retrievable energy⁶ decreases from 4 314 kWh (85,1%), at Cycle 1, to 3 401 kWh (67,1%), at Cycle 24. This decrease represents 18% of useful storage capacity.

⁶ Retrievable energy is considered as the difference between the stored energy after the charge operation and the energy that remains in the TCT after the discharge operation.

Table 2: Stored energy in the TCT considering the theoretical values, the Cycle 1 values, and the Cycle 24 values, in the end of both the charge and discharge operations.

Description	Units	Theoretical Values	Cycle 1 Values	Cycle 24 Values
Charge operation				
Stored energy	[kWh]	5 070,4	4 805,8	4 310,1
	-	-	94,8%	85,0%
Operation time	-	-	2:07:06	1:30:44
Discharge operation				
Stored energy	[kWh]	0	491,5	908,6
	-	-	9,7%	17,9%
Operation time	-	-	1:54:57	1:30:42
Retrievable energy	[kWh]	5 070,4	4 314,3	3 401,5
	-	-	85,1%	67,1%

An identical effect can be observed regarding the time to complete both the operations. Moreover, not only the time to complete the charge and the discharge operations converge to an almost constant value but they both converge to the same value for both the operations (Figure 4).

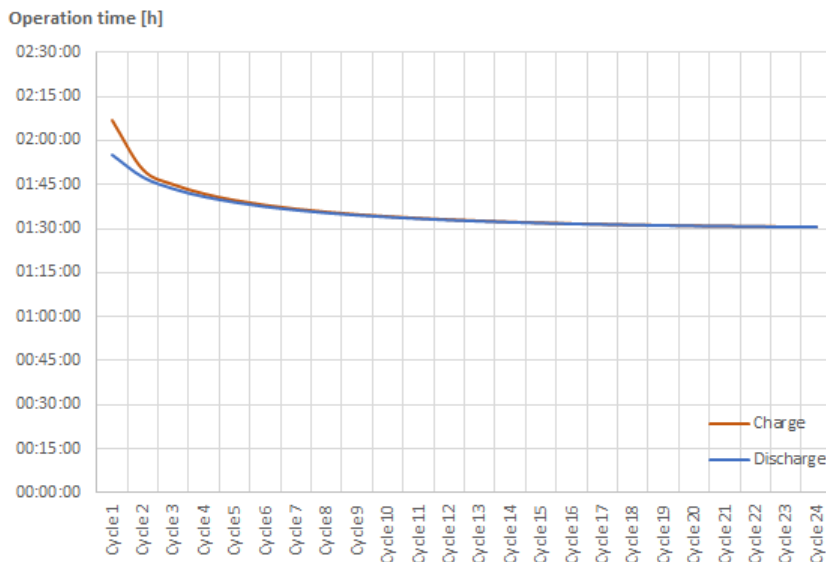


Figure 4: Operation time, for both the charge and the discharge operations, over 24 cycles.

As already presented in Table 2, the effect depicted in both Figure 3 and 4 translates into the decrease of the available thermal capacity in the thermocline, over cycling, which is depicted in Figure 5 and compared to the theoretical storage capacity. From Figure 5, it is possible to verify that the decrease of the mass flow by 60% also decrease the storage capacity. However, this variation is very small.

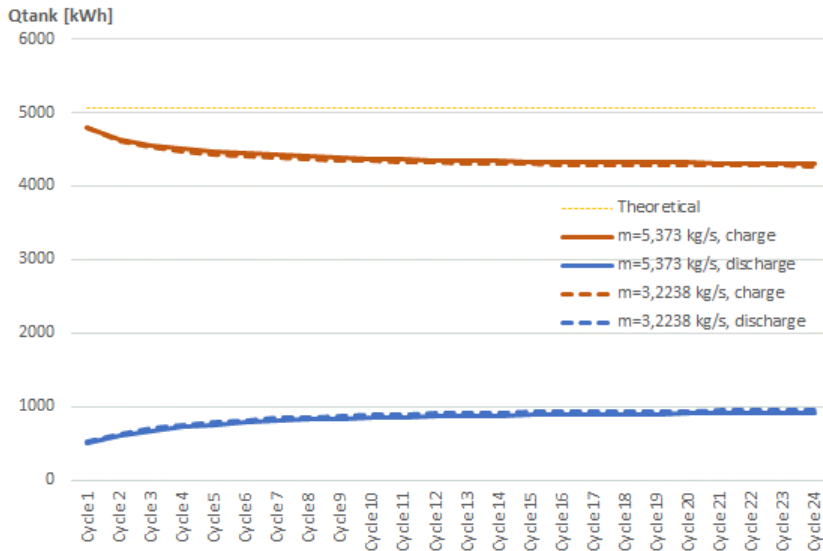


Figure 5: Stored energy vs Cycle number, after charge and discharge operations, for both $m=5,373$ kg/s and $m=3,2238$ kg/s.

Figure 6 shows the outlet temperature plotted over the discharge time for the 24 cycles and the cold temperature (steam generator system return temperature). It can be observed that the temperature of the outlet in the discharge process is constant during most of the discharge operation until it starts decreasing smoothly but increasingly fast. Few minutes later, the discharge ends when the outlet temperature drops by 30 °C.

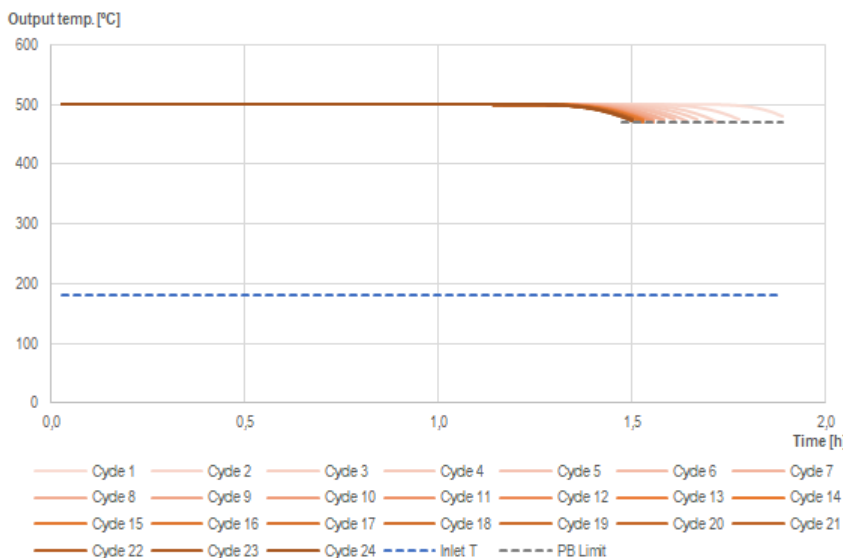


Figure 6: Output temperature for 24 consecutive cycles during the discharge operation ($m=5,373$ kg/s).

When looking into the time, it is possible to observe that the duration of the discharge at the maximum temperature decreases from Cycle 1 to Cycle 24, which was expected considering Figure 4. In this case, the maximum temperature ($T > 499,5 \text{ }^\circ\text{C}$) is maintained for 1h45, at Cycle 1, and to almost 1h17, at Cycle 24. It can also be observed that the same time was found at Cycles 22 to 24. In similar way, the time to decrease temperature in $29,5 \text{ }^\circ\text{C}$ (from $499,5 \text{ }^\circ\text{C}$ to $470 \text{ }^\circ\text{C}$) increases 60% from 8m20s, at Cycle 1, to 13m20s, at Cycles 22 to 24.

4. Prototype TCT performance (alternate strategy)

Looking into the described operation strategy, the TCT appears under exploited, namely due to the threshold limit of $30 \text{ }^\circ\text{C}$ above the minimum temperature ($210 \text{ }^\circ\text{C}$) to end the charge operation, resulting in a poorly charged TCT. Considering that technical limitations exist to a maximum temperature setpoint in the outlet of the charge operation, calculations were performed defining the setpoint as $30 \text{ }^\circ\text{C}$ below the maximum temperature ($470 \text{ }^\circ\text{C}$).

The yielded results highly mitigate the storage capacity decrease with the increase of the operating cycles. Now, the consecutive charging/discharging cycles of the TCT present a rather small impact to the internal temperature profile along time, keeping the thermocline depth and, therefore, its ability to deliver heat over a minimum temperature threshold at the power block inlet.

The effect is now depicted in Figure 7, with the temperature profiles along the axial axis of the TCT overlapping over the course of 12 charging/discharging cycles. The analysis of the present approach was only considered for 12 cycles. However, it is possible to verify that 3 or 4 cycles are enough to converge the profiles and the amounts of energy stored in the TCT.

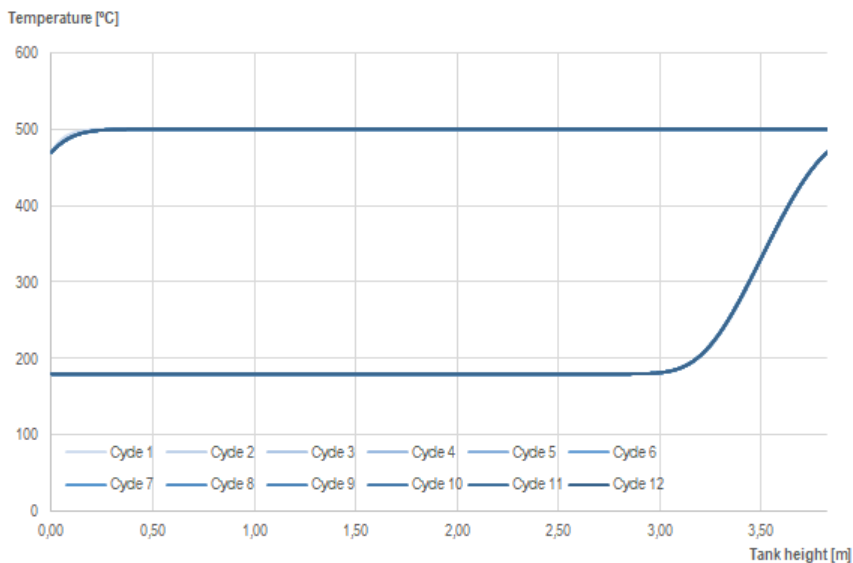


Figure 7: Temperature profiles along the axial axis of the TCT over the course of 12 charging/discharging cycles.

In fact, the same behavior can be found with regard to the time to complete both the operations. Now the time of the charge operation takes 3 to 4 cycles to converge but the discharge operation time does not change since Cycle 1. It is also worth notice that the time of both operations do not converge to the same value, as denoted for the previous described operating strategy (Figure 8).

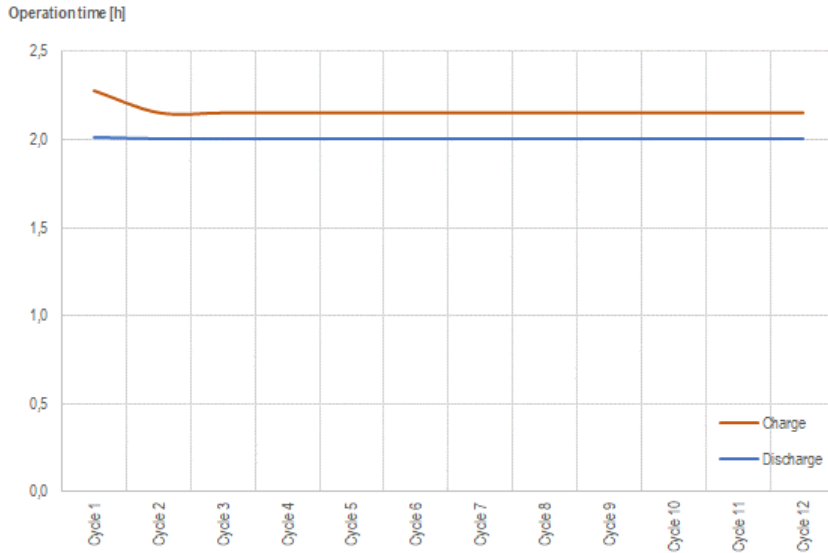


Figure 8: Operation time, for both the charge and the discharge operations, over 12 cycles.

Table 3 presents the stored energy in the TCT considering the theoretical values, the Cycle 1 values, and the Cycle 12 values, in the end of both the charge and discharge operations. From Table 3 is now possible to verify that, even without recycling the TCT, the retrievable energy⁶ has a small decrease from 4 538 kWh (89,5%), at Cycle 1, to 4 531 kWh (89,4%), at Cycle 12. Now, this decrease represents only 0,1% of useful storage capacity and it is much more aligned with the expected behavior of the TCT.

Table 3: Stored energy in the TCT considering the theoretical values, the Cycle 1 values, and the Cycle 12 values, in the end of both the charge and discharge operations.

Description	Units	Theoretical Values	Cycle 1 Values	Cycle 12 Values
Charge operation				
Stored energy	[kWh]	5 070,4	4 974,2	4 971,4
	-	-	98,1%	98,0%
Operation time	-	-	2:16:34	0:08:52
Discharge operation				
Stored energy	[kWh]	0	436,0	440,3
	-	-	8,6%	8,7%
Operation time	-	-	2:00:50	2:00:39
Retrievable energy	[kWh]	5 070,4	4 538,2	4 531,1
	-	-	89,5%	89,4%

As already presented in Table 3, the effects depicted in both Figure 7 and 8 do not translates into any significant decrease of the available thermal capacity in the TCT, over cycling, as depicted in Figure 9. When compared to the theoretical storage capacity, the effective thermal capacity of the TCT is now much more aligned. Considering the very small changes shown on Figure 5 due to mass flow variation, no additional mass flow was tested with this operation strategy.

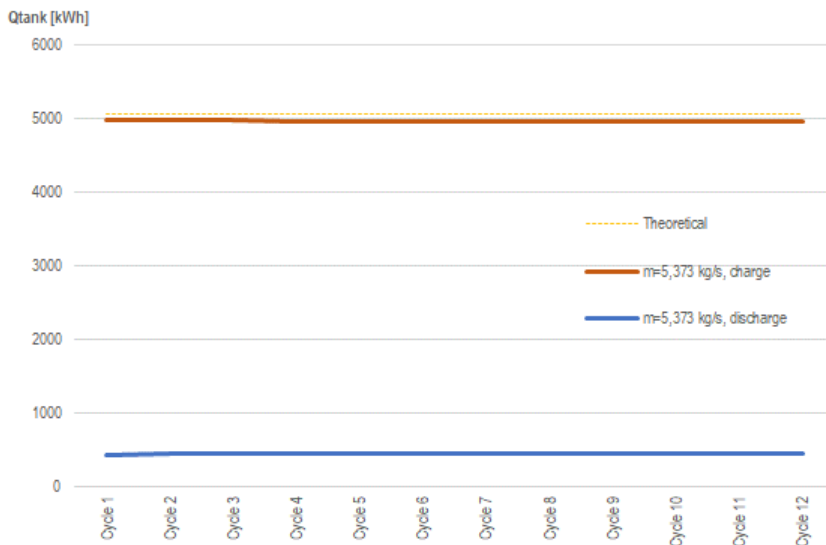


Figure 9: Stored energy vs Cycle number, after charge and discharge operations, for $m=5,373$ kg/s.

Figure 10 shows the outlet temperature plotted over the discharge time for the 12 cycles and the cold temperature (steam generator system return temperature). As reported in Figure 6, it can be observed that the temperature of the outlet in the discharge process is constant during most of the discharge operation until it starts decreasing smoothly but increasingly fast. Few minutes later, the discharge ends when the outlet temperature drops by 30 °C.

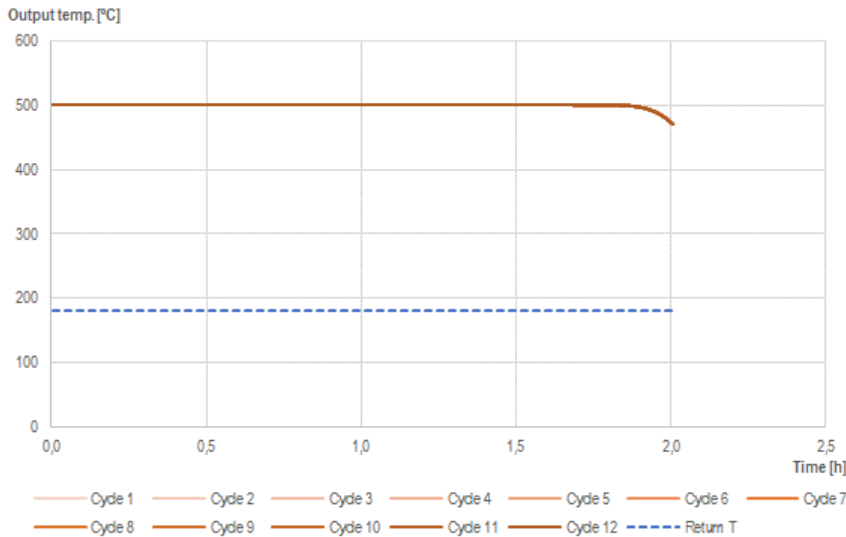


Figure 10: Output temperature for 12 consecutive cycles during the discharge operation ($m=5,373$ kg/s).

However, several differences can be found between Figures 6 and 10. Now, it is not possible to observe the decrease in duration of the discharge operation, from Cycle 1 to Cycle 12. Thus, the maximum temperature ($T > 499,5$ °C) is maintained for 1h51, at Cycle 1, and to 1h50, at Cycle 12. Identically, the time to decrease temperature in 29,5 °C (from 499,5 °C to 470 °C) presents a small increase (6,8%) from 9m50s, at Cycle 1, to 10m30s, at Cycle 12.

Despite the analysis being made between Cycle 1 and 12, from Cycle 5 all Cycles presented the same results as described to Cycle 12.

5. Upscaled TCT performance (alternate strategy)

Considering the prototype TCT and the design options of D7.9, an upscaled TCT was defined. The main specifications are described in Table 4. The Heat Storage Material (HSM) is composed by Solar Salt, used as Heat Thermal Fluid (HTF), and by slag from São Domingos Mines, used as filler material. The thermal properties of Solar Salt, namely density and specific heat, were both retrieved from Serrano/López et al⁷ and the thermal properties for the filler material was already described in D5.1. The thermal energy capacity of the tank was kept considering D7.9. However, a TCT storage

⁷ R. Serrano-López et al. (2013), Chemical Engineering and Processing 73 (2013) 87– 102

efficiency was considered and the TCT capacity was slightly increased and using Equation 1, the compensated volume of the TCT was calculated.

Table 4: Main specifications for the upscaled TCT.

Description	Symbol	Units	Value
Autonomous work time	t_{TES}	[h]	9
Design thermal capacity	Q_{TES}	[MWh]	1233,2
Storage efficiency	η_{TES}	-	98%
Compensated thermal capacity	Q_{CTES}	[MWh]	1258,4
Tank height	h_{HSM}	[m]	10
Tank internal diameter	\emptyset_{HSM}	[m]	29,73
Maximum temperature	T_{max}	[°C]	565
Minimum temperature	T_{min}	[°C]	290
Local porosity	ϵ_{local}	[%]	50
Global porosity Error! Bookmark not defined.	ϵ_{global}	[%]	67,23

$$V_{HSM} = \frac{Q_{CTES}}{(1 - \epsilon) \cdot \rho_{slag} \cdot Cp_{slag} \cdot (T_{max} - T_{min}) + \epsilon \cdot \rho_{SS} \cdot [Cp_{SS@T_{max}} \cdot T_{max} - Cp_{SS@T_{min}} \cdot T_{min}]} \quad \text{Eq. 1}$$

Where:

V_{HSM} : Volume of the Heat Storage Material (HSM) [m³];

Q_{CTES} : Compensated thermal capacity [kJ];

ϵ : Global porosity [-];

ρ_{slag} : Density of the filler material [kg/m³];

ρ_{SS} : Density of the molten salts [kg/m³];

Cp_{slag} : Specific heat of the filler material [kJ/kg-K];

Cp_{SS} : Specific heat of the molten salts [kJ/kg-K];

T_{max} : Temperature at charged state [°C];

T_{min} : Temperature at discharged state [°C];

Also from D7.9, some considerations on the Height/Diameter ratio were disclosed and a variation below 0,07% was found **Error! Bookmark not defined.** when the tank height was tested in the range of 10m to 14m. Considering the use of a 1D model, the numerical discretization increases

towards a smaller height, decreasing the space-step. Therefore, confirming that the tank diameter was kept below 30m **Error! Bookmark not defined.**, the 10m height was considered.

To run the 1D model, a mass flow rate is needed. However, no reported mass flow rate was found for the discharge operation of the TCT. Thus, Equations 2 and 3 were used to calculate a suitable mass flow rate ($\dot{m}_{SS}=319,8$ kg/s).

$$\dot{Q}_{CTES} = \frac{Q_{CTES}}{t_{TES}} \quad \text{Eq. 2}$$

$$\dot{m}_{SS} = \frac{\dot{Q}_{CTES}}{Cp_{SS@T_{max}} \cdot T_{max} - Cp_{SS@T_{min}} \cdot T_{min}} \quad \text{Eq. 3}$$

Where:

\dot{Q}_{CTES} : Compensated power capacity [kW];

Q_{CTES} : Compensated thermal capacity [kWh];

t_{TES} : Autonomous work time [h];

\dot{m}_{SS} : Solar Salt mass flow rate [kW];

Cp_{SS} : Specific heat of the molten salts [kJ/kg-K];

T_{max} : Temperature at charged state [°C];

T_{min} : Temperature at discharged state [°C];

Furthermore, the operation strategy keeps the cut-off temperature in the charge operation with a setpoint of 30 °C below the maximum temperature. The results are presented below in the same fashion as the ones before.

As expected, the temperature profiles for both the charge and the discharge operations appear overlapped after several cycles, as in the prototype TCT (Figure 11). For the simulations of this TCT, only 6 cycles were needed to ensure the convergence of the results. This was needed to soften the computational effort, considering that, in the upscaled TCT, a 9h operations were expected unlike in the prototype TCT, where roughly 2h operations were verified.

The effect is now depicted in Figure 11, with the temperature profiles along the axial axis of the upscaled TCT overlapping over the course of 6 charging/discharging cycles. Despite the analysis of the present approach only considered 6 cycles, it is possible to verify that 3 cycles are enough to converge the profiles and the amounts of energy stored in the TCT.

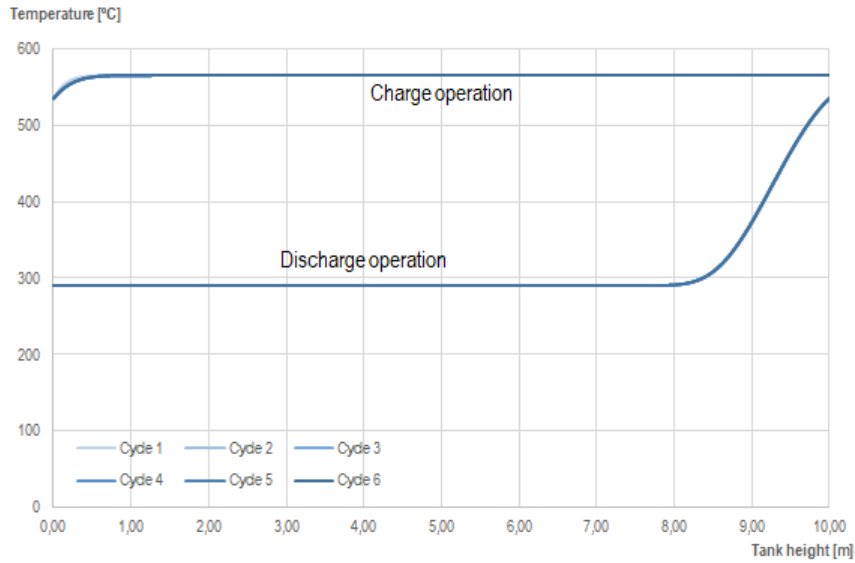


Figure 11: Temperature profiles along the axial axis of the upscaled TCT over the course of 6 charging/discharging cycles.

In fact, the same behavior can be found with regard to the time to complete both the operations. Now the time of the charge operation takes 3 cycles to converge but the discharge operation time does not change since Cycle 1. It is also worth notice that the time of both operations do not converge to the same value, just as verified for the prototype TCT with the same operation strategy, as denoted for the operating strategy described D7.9 (Figure 12).

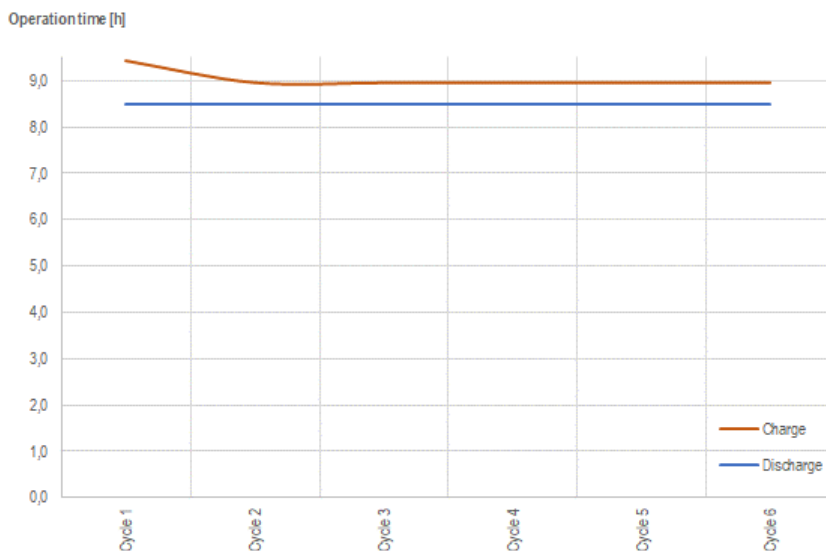


Figure 12: Operation time, for both the charge and the discharge operations, over 6 cycles.

Table 5 presents the stored energy in the upscaled TCT considering the theoretical values, the Cycle 1 values, and the Cycle 6 values, after both the charge and discharge operations. From Table 5 it is possible to verify that, even without recycling the TCT, the retrievable energy has negligible

decrease from 1 138 MWh (86,9%), at Cycle 1, to 1 136 MWh (86,8%), at Cycle 6. This decrease represents 0,1% of useful storage capacity and, just like in the prototype TCT model, it is much more aligned with the expected behavior of the TCT.

Table 5: Stored energy in the upscaled TCT considering the theoretical values, the Cycle 1 values, and the Cycle 6 values, after both the charge and discharge operations.

Description	Units	Theoretical Values	Cycle 1 Values	Cycle 6 Values
Charge operation				
Stored energy	[MWh]	1 309,3	1 228,2	1 227,4
	-	-	93,8%	93,8%
Operation time	-	-	9:25:36	8:57:17
Discharge operation				
Stored energy	[MWh]	0	0,0903	0,0913
	-	-	6,9%	7,0%
Operation time	-	-	8:29:10	8:28:26
Retrievable energy	[MWh]	1 309,3	1 137,9	1 136,2
	-	-	86,9%	86,8%

As presented in Table 5, the effects depicted in both Figure 11 and 12 do not translates into any significant decrease of the available thermal capacity in the upscaled TCT, over cycling. This is clearly perceived in Figure 13. When compared to the upscaled theoretical storage capacity, the effective thermal capacity of the upscaled TCT is well aligned.

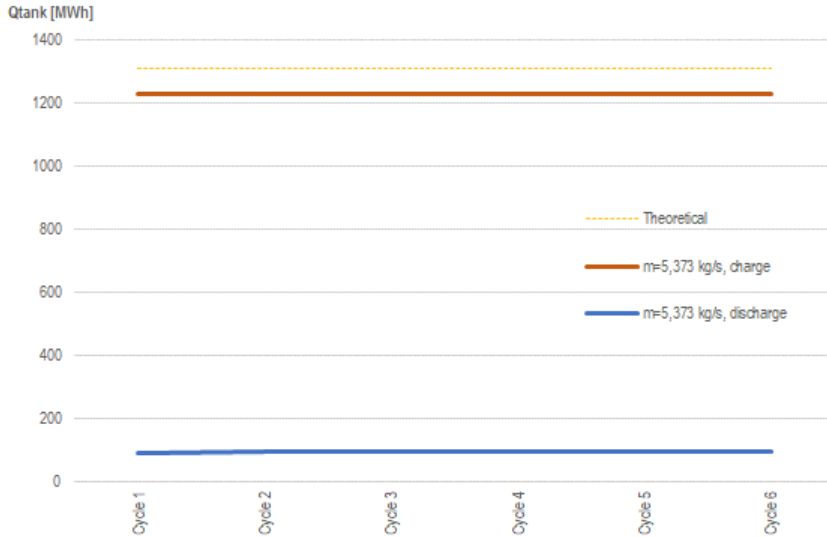


Figure 13: Stored energy vs Cycle number, after charge and discharge operations, for $m=319,8$ kg/s.

Figure 14 shows the outlet temperature plotted over the discharge time for the 6 cycles and the cold temperature (steam generator system return temperature). Again, as reported in Figures 6 and 10, it can be observed that the temperature of the outlet in the discharge process is constant during most of the discharge operation until it starts decreasing smoothly but increasingly fast. Few minutes later, the discharge ends when the outlet temperature drops by 30 °C.

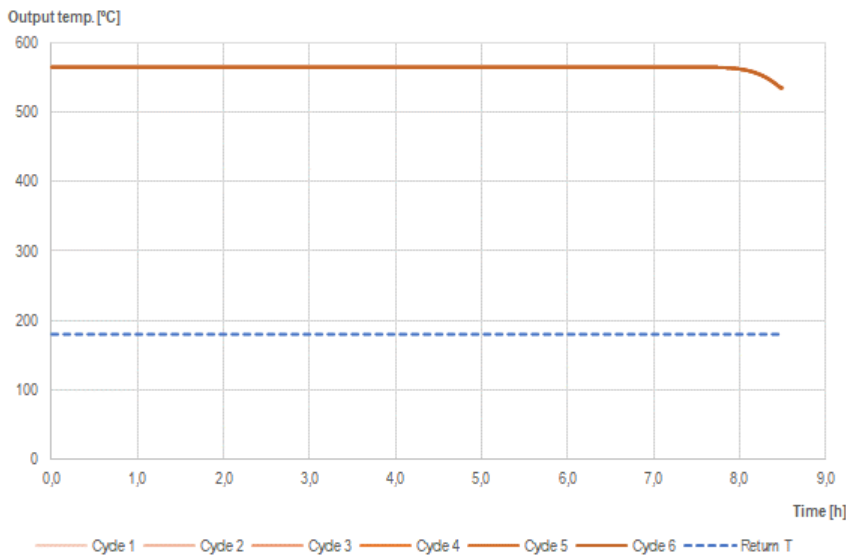


Figure 14: Output temperature for 6 consecutive cycles during the discharge operation ($m=319,8$ kg/s).

From Figure 14 is not possible to observe the decrease in duration of the discharge operation, from Cycle 1 to Cycle 6. Thus, the maximum temperature ($T>564,5$ °C) is maintained for 7h48m40s, at Cycle 1, and to 7h45m10s, at Cycle 6. Identically, the time to decrease temperature in $29,5$ °C (from $564,5$ °C to 535 °C) presents a small increase (6,9%) from 41m20s, at Cycle 1, to 44m10s, at Cycle 6.

Despite the analysis being made between Cycle 1 and 6, from Cycle 3 all Cycles presented the same results as described to Cycle 6.

6. System Advisory Model (SAM)

In D7.9, CSP plant simulations have been performed with the software System Advisory Model (SAM) v2013.9.20³. SAM is a freely available and flexible tool maintained by the U.S. National Renewable Energy Laboratory (NREL). This tool is able to simulate the technical and financial performance of CSP plants, implementing most of the recommendations from the SolarPACES Guideline for Bankable STE Yield Assessment ⁸.

However, SAM presented some shortcomings that resulted in simulations and their respective results with potential to be improved, namely:

- The annual based 1-D model available in SAM yield simulation results that do not account for the cycling effect over the effective thermal capacity of the TCT;
- The 1-D TCT model available in SAM does not account for differentiated local values of porosity. Instead, a weighted average value for porosity must be calculated prior to the use of the application and a global porosity for all the control volume must be considered; and
- Due to reported limitations of the application, for discharge outlet temperature values greater than 450 °C, the simulations failed to converge. Therefore, this set-point value was considered in all simulations, instead of the proposed threshold temperature of 535 °C for the upscaled TCT.

Eventually, the use of TRNSYS⁹ would be able to improve the results presented by SAM, namely with regard to the threshold temperature of 535 °C for the upscaled TCT.

For the TCT model-specific limitations in SAM, the available libraries for TRNSYS also miss the accounting of the cycling effect and the definitions of “zones” with different porosity values. Otherwise, TRNSYS allows the computation of user developed equations that can address this issue or, alternatively, allows the development of a computational component (Type) that includes parameters for cycling the TCT and to consider the local porosity in one or more specific zones.

7. Conclusions

This report approaches the problem of the thermocline tank (TCT) degradation that can develop after consecutive cycles, under the proposed operation strategy.

⁸ D. Kesseli, M. Wagner, R. Guédez, and C. S. Turchi, “CSP-plant modeling guidelines and compliance of the system advisor model (SAM),” AIP Conf. Proc., vol. 2126, no. July, 2019.

⁹ Klein, S.A. et al (2017). TRNSYS 18: A Transient System Simulation Program, Solar Energy Laboratory, University of Wisconsin, Madison, USA, <http://sel.me.wisc.edu/trnsys>

Calculations were performed towards the assessment of the prototype TCT performance considering the proposed operation strategy.

The assessment revealed that the stored energy during Cycle 1 is not representative of continuous utilization of the TCT and only after more than 20 charge and discharge cycles the TCT operation converges to a given performance, decreasing significantly the TCT useful storage capacity from 85,1% to 67,1% (the reference is the theoretical useful storage capacity).

An alternate operation strategy was proposed, and its performance assessed. The proposed operating strategy changes the set-point temperature for the charge operation from $T_{min}+30$ °C to $T_{max}-30$ °C (in the prototype TCT the set-point temperature changes from 210 °C to 470 °C).

With the alternate operation strategy, the TCT useful storage capacity yields 89,5% in Cycle 1 and decreases slightly to 89,4% in Cycle 12. Moreover, the temperature profiles converge after 5 cycles instead the 20 cycles previously reported.

An upscaled TCT was assessed using the alternate operation strategy. Besides the size, it also introduced some additional differences, namely the height/diameter ratio, from 1,32 to 0,34, the heat transfer fluid, from Yara MOST to Solar Salt, and the number of available autonomous hours, from 2h~3h (depending on the mass flow rate) to 9h.

The calculations performed with the upscaled TCT yielded 86,9% in Cycle 1 and 86,8% in Cycle 6. For this analysis, the temperature profiles were fully converged after 3 cycles. It's worth noting that the decrease found in Cycle 1 when compared to Cycle 1 of prototype TCT under the same operation strategy is largely related to the decrease in the H/D ratio. The positive or negative influence of the HTF thermal properties was not assessed.

Although System Advisory Model (SAM) can be used to simulate the technical and financial performance of CSP plants, some thermocline model related shortcomings hinder the yielded results. Two were found related with the definition of the model itself, namely the absence of the cycling effect and the possibility to define the porosity parameters locally, and one related with numerical divergence.

Eventually, the upscaled solution presented in D7.9 would benefit from a more thorough analysis performed in a more versatile computational environment such as TRNSYS. Even without the financial part, TRNSYS would allow for a calibration of SAM's model.

Finally, the alternate operation strategy yielded improved results when compared with the proposed operation strategy presented in D7.9.

Furthermore, considering the improvement found with the alternate operating strategy, recycling the TCT in the end of each charge operation would not significantly improve the performance of the TCT. This is known by the negligible decrease in useful storage capacity after the convergence of the temperature profiles after consecutive cycles.